Mem. Fac. Eng., Osaka City Univ., Vol. 39, pp. 53－69 (1998)

Fundamental Theory of Computer Program, EPASS, for Applying Elasto-Plastic and Finite Displacement Analysis to Spatial Framed Steel Bridges

Toshiyuki KITADA[1], Hiroshi NAKAI[2] and Katsuhiro TANAKA[3]

(*Received September* 30, 1998)

Synopsis: Described in this paper is the fundamental theory of a computer program, EPASS, which have been developed for the elasto-plastic and finite displacement analysis of spatial framed steel bridge structures composed of the thin-walled box members and cable members by taking strain hardening of steel materials into consideration. An efficient formulation for the elasto-plastic and finite displacement theory of the thin-walled box members subjected to the combinations of bending, compression and torsion is presented. Then, some effective strategies for nonlinear analysis such as the arc-length method, technique by using current stiffness parameter and under-relaxation method are employed in the theory for making the accurate evaluation of the ultimate load carrying capacity of bridge structures. The validity of this proposed methods is demonstrated through the analyses of various numerical examples and an actual cable-stayed bridge.

Keywords: Elasto-plastic and finite displacement analysis, Ultimate strength, Finite element method, Three dimensional framed structure, Steel bridge

1. Introduction

In recent years, numerous long span and complicated steel bridges, such as the Akashi-kaikyo bridge, a suspension bridge with the longest span in the world, and Tatara bridge, a cable-stayed bridge with also the longest span in the world, have been constructed according to the development of design techniques and manufacturing skills in Japan. In the design of such bridges, it is one of the most important works to estimate their ultimate load carrying capacity from a standpoint of limit state, particularly, ultimate limit state. Some computer programs[1)-3)] for calculating the ultimate strength of three dimensional framed structures on the basis of the elasto-plastic and finite displacement theory have already been developed hitherto. Among them, several finite element programs for solving the comprehensive problems, such as ABAQUS, MARC and NASTRAN can, of course, be used for this purpose. However, these programs may not cope with various and sophisticated problems on the analysis of practical and spatial bridge structures, because they are too comprehensive and large. That is the reason why a computer program, EPASS[4), 5)], have been developed for the elasto-plastic and finite displacement analysis of the framed steel bridge structures composed of the thin-walled box members and cable members.

In the EPASS, various theories and analytical techniques are employed according to our experiences. Although the elasto-plastic behavior of the thin-walled box members subjected to bending, compression and torsion simultaneously is formulated on the basis of Komatsu-Sakimoto's method[1)], the stress-strain

[1] Associate Professor, Department of Civil Engineering

[2] Professor, Department of Civil Engineering

[3] Postgraduate Student, Doctor Course, Department of Civil Engineering (Japan Information Processing Service Co., Ltd.)

relationship of steel materials composing the thin-walled box members is not perfectly elasto-plastic but on the combinations of isotropic hardening and kinematic one.

Generally speaking, some difficult problems occur in the elasto-plastic and finite displacement analysis of large and complicated steel bridge structures, for instance, problems that the accurate ultimate load carrying capacity is not often calculated or evaluated exactly. Several effective strategies for adopting nonlinear analysis such as the arc-length method[6),7)], technique by using current stiffness parameter[8)] and under-relaxation method[9),10)] are employed to solve the problems, and the other effective strategies for the analysis of spatial steel bridges are also employed.

First of all, this paper describes the basic formulation of the elasto-plastic and finite displacement theory of the thin-walled box members subjected to the combinations of bending, compression and torsion. Secondly, the outlines of the EPASS and the effective strategies which are used in the EPASS are shown in detail. Several numerical examples are analyzed for investigating the validity of the proposed formulation. Finally, an example of an actual cable-stayed bridge is analyzed to verify the efficiency of the proposed strategies.

2. Elasto-Plastic and Finite Displacement Analysis

2.1 Analytical Assumptions

The elasto-plastic and finite displacement behavior of the thin-walled box members is formulated on the basis of the following assumptions:

1) The finite displacement behavior is formulated according to the Approximate Updated Lagrangian Description (AULD) method[11)].
2) The cross section of the beam-column members keeps plane after deformation.
3) The shearing stress due to flexure and the warping stress due to torsion can be neglected.
4) The torsional angle of the cross section is small enough to be ignored.
5) The elasto-plastic behavior of the thin–walled box members is formulated according to the assumption[1)] of constant shear flow along the box wall even after the partial yielding is occurred in the cross section.
6) The material of the box members is assumed to be homogeneous, isotropic, strain hardening and satisfying the von Mises' yield criterion as well as Prandtl-Reuss' plastic flow rule.
7) The local buckling of the component plates of the box members do not occur.

2.2 Formulation using Principle of Virtual Work

The elasto-plastic and finite displacement behavior of the thin-walled box members is formulated by applying the incremental variational method. When a box beam-column element which stays in the equilibrium configuration of load step n, is subjected to incremental loads and moves to the equilibrium configuration of load step $n+1$, the fundamental equation is obtained from the principle of virtual work as follows:

$$\int_0^l \delta\Delta\boldsymbol{e}^T\left(\boldsymbol{f}^{(n)}+\Delta\boldsymbol{f}\right)dx=\delta\Delta\boldsymbol{u}^T\boldsymbol{p}^{(n+1)} \tag{1}$$

where

$\Delta\boldsymbol{u}$: incremental nodal displacement vector

$\Delta\boldsymbol{e}$: incremental deformation vector

$\boldsymbol{f}^{(n)}$: stress-resultant vector at the configuration of load step n

$\Delta\boldsymbol{f}$: incremental stress-resultant vector

$\boldsymbol{p}^{(n+1)}$: nodal force vector including incremental nodal force to the configuration of load step $n+1$

and l, δ and the superscript T denote the length of the element, variation, and transposition of vectors, respectively.

The incremental deformation vector $\Delta\boldsymbol{e}$ is the summation of linear term $\Delta\boldsymbol{e}_L$ and nonlinear term $\Delta\boldsymbol{e}_N$. Thus,

$$\Delta\boldsymbol{e} = \Delta\boldsymbol{e}_L + \Delta\boldsymbol{e}_N \tag{2}$$

While, the incremental stress-resultant vector $\Delta\boldsymbol{f}$ can be expressed as a material rigidity matrix $\boldsymbol{S}$ and the incremental deformation vector $\Delta\boldsymbol{e}$, then

$$\Delta\boldsymbol{f} = \boldsymbol{S}\Delta\boldsymbol{e} = \left(\boldsymbol{S}_e + \boldsymbol{S}_p\right)\left(\Delta\boldsymbol{e}_L + \Delta\boldsymbol{e}_N\right) \tag{3}$$

where $\boldsymbol{S}_e$ and $\boldsymbol{S}_p$ are the elastic and plastic material rigidity matrices, respectively. Substitution of Eqs. (2) and (3) into Eq. (1) gives

$$\int_0^l \delta\left(\Delta\boldsymbol{e}_L + \Delta\boldsymbol{e}_N\right)^T \left(\boldsymbol{S}_e + \boldsymbol{S}_p\right)\left(\Delta\boldsymbol{e}_L + \Delta\boldsymbol{e}_N\right) dx + \int_0^l \delta\Delta\boldsymbol{e}_N^T \boldsymbol{f}^{(n)} dx$$
$$= \delta\Delta\boldsymbol{u}^T \boldsymbol{p}^{(n+1)} - \int_0^l \delta\Delta\boldsymbol{e}_L^T \boldsymbol{f}^{(n)} dx \tag{4}$$

Since the first term of the left-hand side in Eq. (4) is nonlinear term with respect to incremental displacement, Eq. (4) may be reduced approximately to the linear form as follows by neglecting the high order terms:

$$\int_0^l \delta\Delta\boldsymbol{e}_L^T \left(\boldsymbol{S}_e + \boldsymbol{S}_p\right)\Delta\boldsymbol{e}_L dx + \int_0^l \delta\Delta\boldsymbol{e}_N^T \boldsymbol{f}^{(n)} dx = \delta\Delta\boldsymbol{u}^T \boldsymbol{p}^{(n+1)} - \int_0^l \delta\Delta\boldsymbol{e}_L^T \boldsymbol{f}^{(n)} dx \tag{5}$$

The stiffness matrix of the box beam-column element can be derived from Eq. (5) as shown in the latter.

2.3 Relationship between Strains and Displacements

(1) Normal Strain

The local coordinate system of the box beam-column element is situated as shown in Fig. 1. The incremental displacements $(\Delta u_p, \Delta v_p, \Delta w_p)$ at a point $P(x, y, z)$ in the cross section, which are shown in Fig. 2, can be expressed by the incremental displacements $(\Delta u, \Delta v, \Delta w)$ at the shear center and the incremental torsional angel $\Delta\phi$ of the cross section as follows:

$$\left.\begin{aligned}
\Delta u_p &= \Delta u - \left(y\cos\Delta\phi - z\sin\Delta\phi\right)\Delta v' - \left(z\cos\Delta\phi + y\sin\Delta\phi\right)\Delta w' \\
\Delta v_p &= \Delta v - z\sin\Delta\phi - y\left(1 - \cos\Delta\phi\right) \\
\Delta w_p &= \Delta w + y\sin\Delta\phi - z\left(1 - \cos\Delta\phi\right)
\end{aligned}\right\} \tag{6}$$

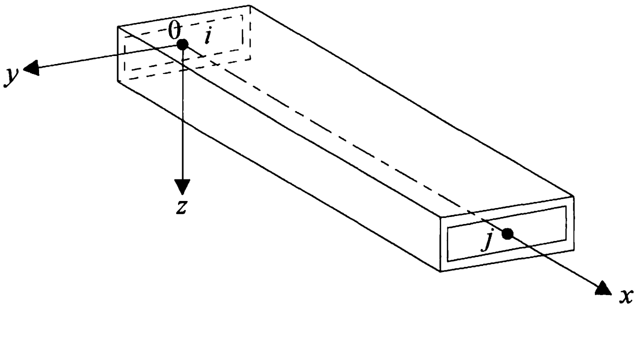

Fig. 1 Box beam-column element and local coordinate system

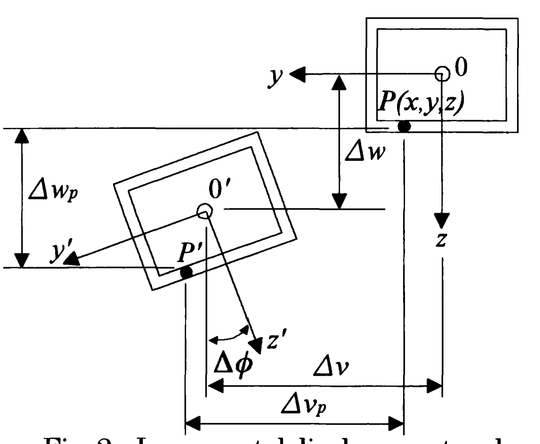

Fig. 2 Incremental displacement and torsional angle of cross section

in which the prime means the derivative with respect to the coordinate axis- x .

The incremental normal strain $\Delta\varepsilon$ at the point P is generally given by

$$\Delta\varepsilon = \Delta u_p' + \frac{1}{2}\left(\Delta v_p'\right)^2 + \frac{1}{2}\left(\Delta w_p'\right)^2 \tag{7}$$

Substitution of Eq. (6) into Eq. (7) gives

$$\Delta\varepsilon = \Delta\varepsilon_0 - y\Delta\psi_z + z\Delta\psi_y + \left(y^2 + z^2\right)\Delta\psi_\phi \tag{8}$$

where $\Delta\varepsilon_0$, $\Delta\psi_z$, $\Delta\psi_y$ and $\Delta\psi_\phi$ are obtained by the assumption that the torsional angle is small enough to be ignored and by neglecting the higher order terms as follows:

$$\left.\begin{aligned}
\Delta\varepsilon_0 &= \Delta u' + \frac{1}{2}\left(\Delta v'\right)^2 + \frac{1}{2}\left(\Delta w'\right)^2 \\
\Delta\psi_z &= \Delta v'' + \Delta\phi\,\Delta w'' \\
\Delta\psi_y &= -\Delta w'' + \Delta\phi\,\Delta v'' \\
\Delta\psi_\phi &= \frac{1}{2}\left(\Delta\phi'\right)^2
\end{aligned}\right\} \tag{9}$$

(2) Shearing Strain

The box beam-column element subjected to pure torsion is deformed as shown in Fig. 3. For this situation, the incremental shearing strain $\Delta\gamma$ at an arbitrary point in the cross section, illustrated in Fig. 4, is given by the sum of the shearing strain due to pure torsion and warping as follows:

$$\Delta\gamma = r_s\Delta\phi' + \frac{\partial\Delta\tilde{u}}{\partial s} = r_s\Delta\theta + \frac{\partial\Delta\tilde{u}}{\partial s} \tag{10}$$

where r_s is the perpendicular distance from the shear center to the center line of the wall under consideration, $\Delta\tilde{u}$ is the incremental displacement due to warping, s is the curvilinear coordinate along the perimeter of the cross section, and $\Delta\theta$ is the rate of incremental torsional angle.

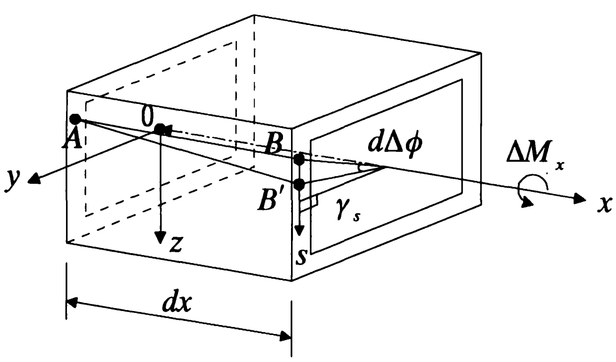

Fig. 3 Deformation of element subjected to pure torsion

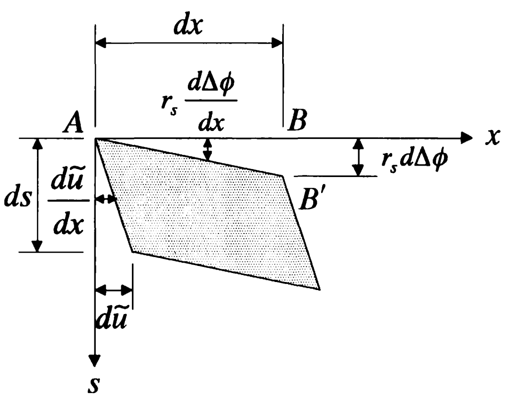

Fig. 4 Deformation of small element $dx \times ds$

2.4 Relationship between Stresses and Strains

(1) Elastic Zone

The relationship between the incremental stresses and incremental strains in the elastic zone of the box beam-column element is expressed by Hooke' s law as follows:

$$\begin{Bmatrix} \Delta\sigma \\ \Delta\tau \end{Bmatrix} = \boldsymbol{D}_e \begin{Bmatrix} \Delta\varepsilon \\ \Delta\gamma \end{Bmatrix} \tag{11}$$

where

$$\boldsymbol{D}_e = \begin{bmatrix} E & 0 \\ 0 & G \end{bmatrix} \tag{12}$$

in which $\Delta\sigma$ and $\Delta\tau$ are the incremental normal stress and incremental shearing stress, and E and G are the Young's modulus and shear modulus of elasticity, respectively.

(2) Plastic Zone

The combination of isotropic hardening and kinematic one on the basis of von Mises' yield criterion is defined by

$$f = \sqrt{(\sigma - \alpha_1)^2 + 3(\tau - \alpha_2)^2} - H(\bar{\varepsilon}_p) = 0 \tag{13}$$

where two parameters α_1 and α_2 are the coordinates of the center of the yield surface, and $H(\bar{\varepsilon}_p)$ means the size of the yield surface which is the function of the equivalent plastic strain $\bar{\varepsilon}_p$. The term of the square root in the above equation means the equivalent stress $\bar{\sigma}$. Thus,

$$\bar{\sigma} = \sqrt{(\sigma - \alpha_1)^2 + 3(\tau - \alpha_2)^2} \tag{14}$$

The incremental equivalent stress, $\Delta\bar{\sigma}$ is obtained from Eq. (13) as follows:

$$\Delta\bar{\sigma} = \frac{(\sigma - \alpha_1)(\Delta\sigma - \Delta\alpha_1) + 3(\tau - \alpha_2)(\Delta\tau - \Delta\alpha_2)}{\bar{\sigma}} = H'\Delta\bar{\varepsilon}_p \tag{15}$$

where H' is the rate of isotropic hardening. The rate of kinematic hardening H_k' is defined as follows:

$$\frac{(\sigma - \alpha_1)\Delta\alpha_1 + 3(\tau - \alpha_2)\Delta\alpha_2}{\bar{\sigma}} = H_k'\Delta\bar{\varepsilon}_p \tag{16}$$

The equations for the transition of the yield surface are expressed according to the Ziegler's kinematic law as follows:

$$\begin{Bmatrix} \Delta\alpha_1 \\ \Delta\alpha_2 \end{Bmatrix} = \frac{H_k'\,\Delta\bar{\varepsilon}_p}{\bar{\sigma}} \begin{Bmatrix} \sigma - \alpha_1 \\ \tau - \alpha_2 \end{Bmatrix} \tag{17}$$

According to the associated flow rule, the incremental plastic strains are proportional to the gradient of the yield surface with respect to the corresponding stresses. Thus,

$$\Delta\varepsilon_p = \Delta\lambda \frac{\partial f}{\partial \sigma}, \quad \Delta\gamma_p = \Delta\lambda \frac{\partial f}{\partial \tau} \tag{18}$$

where $\Delta\lambda$ is a scalar which is taken as a positive value or zero.

The incremental plastic work ΔW_p is defined as follows:

$$\Delta W_p = (\sigma - \alpha_1)\Delta\varepsilon_p + (\tau - \alpha_2)\Delta\gamma_p = \bar{\sigma}\Delta\bar{\varepsilon}_p \tag{19}$$

Since each incremental strain at the plastic state is the summation of the incremental elastic strain and plastic one, Eq. (11) can be rewritten as follows:

$$\begin{Bmatrix}\Delta\sigma\\ \Delta\tau\end{Bmatrix} = \boldsymbol{D}_e \begin{Bmatrix}\Delta\varepsilon - \Delta\varepsilon_p\\ \Delta\gamma - \Delta\gamma_p\end{Bmatrix} \tag{20}$$

From Eqs. (15), (16), (18), (19) and (20), $\Delta\lambda$ is derived as follows:

$$\Delta\lambda = \Delta\bar{\varepsilon}_p = \frac{\bar{\sigma}}{S}(S_1\Delta\varepsilon + S_2\Delta\gamma) \tag{21}$$

where

$$S_1 = E(\sigma - \alpha_1)\,,\ \ S_2 = 3G(\tau - \alpha_2) \tag{22}$$

$$S = (H' + H_k')\bar{\sigma}^2 + S_1(\sigma - \alpha_1) + 3S_2(\tau - \alpha_2) \tag{23}$$

Hence, the relationship between the incremental stresses and incremental strains in the plastic zone of the box beam-column element is given by

$$\begin{Bmatrix}\Delta\sigma\\ \Delta\tau\end{Bmatrix} = \boldsymbol{D}_p \begin{Bmatrix}\Delta\varepsilon\\ \Delta\gamma\end{Bmatrix} \tag{24}$$

where

$$\boldsymbol{D}_p = \boldsymbol{D}_e - \frac{1}{S}\begin{bmatrix} S_1{}^2 & S_1S_2\\ S_1S_2 & S_2{}^2\end{bmatrix} \tag{25}$$

(3) Elasto-Plastic Torsion of Box Element

Let us consider that relationship between the stresses and strains in the box beam-column element. For the elastic zone, the incremental shearing strain $\Delta\gamma$ is obtained from Eq. (11) as follows:

$$\Delta\gamma = \frac{\Delta\tau}{G} \tag{26}$$

The corresponding incremental normal stress, $\Delta\sigma$ being given by

$$\Delta\sigma = E\,\Delta\varepsilon \tag{27}$$

For the plastic zone, the incremental shearing strain $\Delta\gamma$ is obtained from Eq. (24) as follows:

$$\Delta\gamma = \frac{\Delta\tau}{G} + S_h\left[\frac{3(\tau - \alpha_2)}{\sigma - \alpha_1}\right]^2\frac{\Delta\tau}{E} + S_h\frac{3(\tau - \alpha_2)}{\sigma - \alpha_1}\Delta\varepsilon \tag{28}$$

where

$$S_h = \frac{E(\sigma - \alpha_1)^2}{(H' + H_k')\bar{\sigma}^2 + E(\sigma - \alpha_1)^2} \tag{29}$$

The corresponding incremental normal stress, $\Delta\sigma$ being given by

$$\Delta\sigma = E\,\Delta\varepsilon - S_hE\Delta\varepsilon - S_h\frac{3(\tau - \alpha_2)}{\sigma - \alpha_1}\Delta\tau \tag{30}$$

Substitution of Eqs. (26) and (28) into Eq. (10) and integration around the perimeter of the cross section results in

$$\frac{1}{G}\int_e \Delta\tau ds + \frac{1}{G}\int_p \Delta\tau ds + \frac{1}{E}\int_p S_h\left[\frac{3(\tau - \alpha_2)}{\sigma - \alpha_1}\right]^2\Delta\tau ds + \int_p S_h\frac{3(\tau - \alpha_2)}{\sigma - \alpha_1}\Delta\varepsilon ds = \Delta\theta\oint r_s ds + \oint\frac{\partial\Delta\tilde{u}}{\partial s}ds \tag{31}$$

where $\int_e ds$ and $\int_p ds$ mean the integration along the elastic and plastic zone, respectively and $\oint ds$ is the integration around the perimeter of the section. The second term of the right-hand side in Eq. (31) vanishes because of the continuity condition of warping in the box cross section.

Substituting Eq. (8) into Eq. (31) and assuming constant shear flow in the box cross section, the incremental shearing flow Δq can be derived as follows:

$$\Delta q = \Delta\tau \cdot t = -\frac{1}{C_1 + C_2}\left(C_3\Delta\varepsilon_0 - C_4\Delta\psi_z + C_5\Delta\psi_y + C_6\Delta\psi_\phi - C_7\Delta\theta\right) \tag{32}$$

where t is the thickness of the component plates of the box beam-column element and

$$\left.\begin{aligned}
C_1 &= \frac{1}{G}\oint\frac{1}{t}ds, & C_2 &= \frac{1}{E}\int_p S_h\left[\frac{3(\tau-\alpha_2)}{\sigma-\alpha_1}\right]^2\frac{1}{t}ds,\\
C_3 &= \int_p S_h\frac{3(\tau-\alpha_2)}{\sigma-\alpha_1}ds, & C_4 &= \int_p S_h\frac{3(\tau-\alpha_2)}{\sigma-\alpha_1}yds,\\
C_5 &= \int_p S_h\frac{3(\tau-\alpha_2)}{\sigma-\alpha_1}zds, & C_6 &= \int_p S_h\frac{3(\tau-\alpha_2)}{\sigma-\alpha_1}\left(y^2+z^2\right)ds,\\
C_7 &= \oint r_s ds = 2A_s
\end{aligned}\right\} \tag{33}$$

in which A_s is the area enclosed by the center line of the wall in the box cross section.

Substituting Eq. (32) into Eq. (30), the relationship between the incremental normal stress and incremental stains in the plastic zone can be obtained as follows:

$$\begin{aligned}\Delta\sigma &= E\Delta\varepsilon - S_h E\Delta\varepsilon\\
&\quad + S_h\frac{3(\tau-\alpha_2)}{\sigma-\alpha_1}\frac{1}{C_1+C_2}\left(C_3\Delta\varepsilon_0 - C_4\Delta\psi_z + C_5\Delta\psi_y + C_6\Delta\psi_\phi - C_7\Delta\theta\right)\end{aligned} \tag{34}$$

2.5 Relationship between Stress-Resultants and Strains

The incremental stress-resultants of the box beam-column element can be expressed by integrating the incremental normal stress $\Delta\sigma$ and the incremental shearing flow Δq in the cross section. The positive sign of the stress-resultants is defined as shown in Fig. 5, and then the corresponding incremental stress-resultants are given by

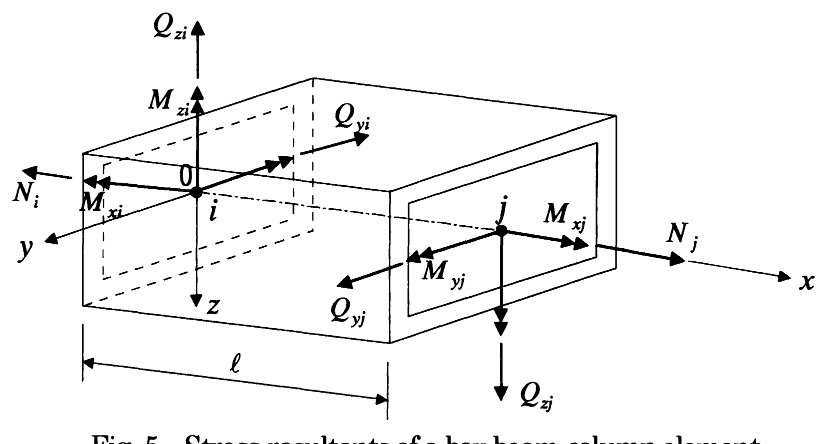

Fig. 5 Stress-resultants of a box beam-column element

$$\left.\begin{aligned}
\Delta N &= \int_A \Delta\sigma\, dA = \int_e \Delta\sigma\, dA + \int_p \Delta\sigma\, dA \\
\Delta M_z &= -\int_A \Delta\sigma\, y dA = -\int_e \Delta\sigma\, y dA - \int_p \Delta\sigma\, y dA \\
\Delta M_y &= \int_A \Delta\sigma z dA = \int_e \Delta\sigma z dA + \int_p \Delta\sigma z dA \\
\Delta M_p &= \int_A \Delta\sigma\left(y^2+z^2\right) dA = \int_e \Delta\sigma\left(y^2+z^2\right) dA + \int_p \Delta\sigma\left(y^2+z^2\right) dA \\
\Delta M_x &= \oint \Delta q r_s ds
\end{aligned}\right\} \tag{35}$$

Substituting Eqs. (8), (27), (32) and (34) into Eq. (35), the final equation can be written in a matrix form as follows:

$$\Delta \boldsymbol{f} = (\boldsymbol{S}_e + \boldsymbol{S}_p)\Delta \boldsymbol{e} \tag{36}$$

where

$$\Delta \boldsymbol{f} = \left\{\Delta N \quad \Delta M_z \quad \Delta M_y \quad \Delta M_p \quad \Delta M_x\right\}^T \tag{37}$$

$$\Delta \boldsymbol{e} = \left\{\Delta\varepsilon_0 \quad \Delta\psi_z \quad \Delta\psi_y \quad \Delta\psi_\phi \quad \Delta\theta\right\}^T \tag{38}$$

$$\boldsymbol{S}_e = \begin{bmatrix} EA_e & & & & \\ -ES_z & EI_z & & Sym. & \\ ES_y & -EI_{yz} & EI_y & & \\ E\left(I_z+I_y\right) & -EI_{py} & EI_{pz} & EI_{pp} & \\ 0 & 0 & 0 & 0 & GJ \end{bmatrix} \tag{39.a}$$

$$\boldsymbol{S}_p = \frac{1}{C_1+C_2}\begin{bmatrix} C_3^2 & & & & \\ -C_3C_4 & C_4^2 & & Sym. & \\ C_3C_5 & -C_4C_5 & C_5^2 & & \\ C_3C_6 & -C_4C_6 & C_5C_6 & C_6^2 & \\ -C_3C_7 & C_4C_7 & -C_5C_7 & -C_6C_7 & -GJC_2 \end{bmatrix} \tag{39.b}$$

in which

$$\left.\begin{aligned}
&A_e = \int_A dA - \int_p S_h dA, \qquad S_z = \int_A y dA - \int_p S_h y dA, \\
&S_y = \int_A z dA - \int_p S_h z dA, \qquad I_z = \int_A y^2 dA - \int_p S_h y^2 dA, \\
&I_y = \int_A z^2 dA - \int_p S_h z^2 dA, \quad I_{yz} = \int_A yz dA - \int_p S_h yz dA, \\
&I_{py} = \int_A \left(y^2+z^2\right) y dA - \int_p S_h \left(y^2+z^2\right) y dA, \\
&I_{pz} = \int_A \left(y^2+z^2\right) z dA - \int_p S_h \left(y^2+z^2\right) z dA, \\
&I_{pp} = \int_A \left(y^2+z^2\right)^2 dA - \int_p S_h \left(y^2+z^2\right)^2 dA, \\
&J = \frac{4A_s^2}{\oint \frac{1}{t}} ds
\end{aligned}\right\} \tag{40}$$

2.6 Equilibrium Equation

By using Eq. (5) on the tangent stiffness matrix, the following equilibrium equation can be derived for an elasto-plastic box beam-column element expressed in their local coordinate system:

$$\left(\boldsymbol{k}_e + \boldsymbol{k}_p + \boldsymbol{k}_g\right) \Delta \boldsymbol{u} = \boldsymbol{p} - \boldsymbol{f}_I \tag{41}$$

where $\boldsymbol{k}_e$, $\boldsymbol{k}_p$, $\boldsymbol{k}_g$, and $\boldsymbol{f}_I$ are the elastic stiffness matrix, plastic stiffness matrix, geometric stiffness matrix, and the nodal force vector for the internal forces, respectively.

Equation (41) should be transformed to the global coordinate system through their transformation matrix $\boldsymbol{T}$ and the whole equilibrium equation in the global coordinate system can easily be obtained by assemblying the transformed equation of all the elements.

3. Outline of EPASS

EPASS is a computer program which have been developed for the elasto-plastic and finite displacement analysis of spatial framed steel bridge structures composed of the thin-walled box members and cable members. By using the EPASS, it may be possible to estimate the ultimate load carrying capacity of the Nielsen-Lohse arch bridges, cable-stayed bridges, suspension bridges and other special types of bridges.

The main features of the program are outlined as follows:

1) The various finite elements and connections can be adopted, as listed in Table 1.
2) The choice of elastic or elasto-plastic analysis and small or finite displacement analysis is possible according to analytical purposes.
3) The elasto-plastic behavior of the thin-walled box members subjected to the combinations of bending, compression and torsion can be simulated on the basis of the theory described in Chapter 2.
4) An arbitrary cross-sectional shape including box cross section with multi-cells can be treated in the elasto-plastic box beam-column element. However, the shearing flow is assumed to flow along only the outside perimeter of the cross section.
5) The inherent residual stress and initial deflection in the steel bridge members can be taken into consideration.
6) The non-linearity of cable members due to cable tension can be accounted according to the tangent stiffness equation of catenary cables on the basis of the Goto's method[12].

Table 1 Types of finite elements and connections in EPASS

(a) Finite elements

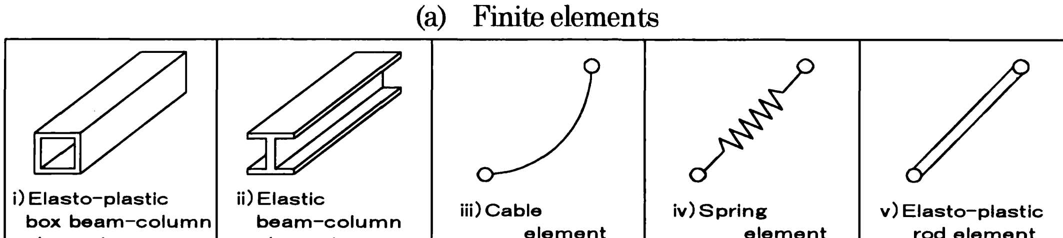

(b) Connections

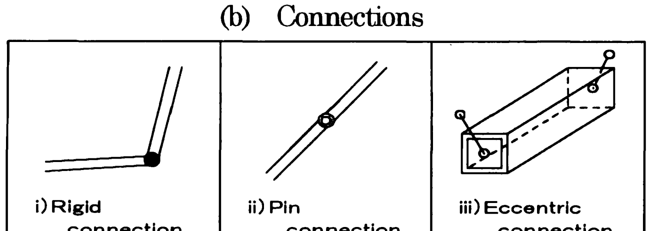

7) All kinds of load combinations used in bridge design can be adopted.
8) The initial stress-resultants and loads for the initial configuration of an analytical model can easily be taken into consideration.
9) The equilibrium path of the analytical model after their ultimate load point can be traced.

A system surrounding the EPASS is illustrated in Fig. 6. This system consists of pro-processing programs for making the initial configuration of the bridge structure, main program EPASS and post-processing programs for representing the numerical results diagrammatically.

In one of the pre-processing programs, the stress-resultants in the structural members of an analytical model subjected to dead load and prestressing load are calculated by the elastic linear analysis in advance of the elasto-plastic and finite displacement analysis. The calculated stress-resultants are inputted into the EPASS as the initial ones, so that the expected initial configuration of the analytical model can easily be generated. The most unfavorable initial deflection of the analytical model can be evaluated according to the fundamental buckling mode calculated by a pre-processing buckling analysis.

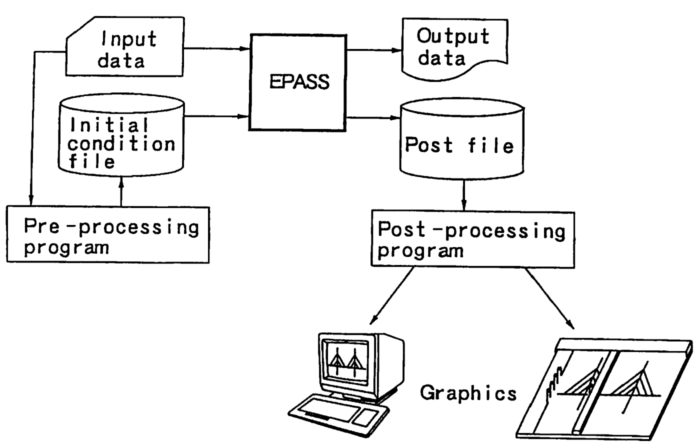

Fig. 6 System surrounding EPASS

4. Effective Strategies for Analysis of Spatial Steel Bridges

There are some effective strategies which are used in the EPASS for the accurate and efficient evaluation of the ultimate load carrying capacity as well as reduction of computation time. For these strategies, arc-length method, technique by using the current stiffness parameter and under-relaxation method are introduced mainly as follows.

4.1 Arc-Length Method

To evaluate an unknown ultimate load by the load incremental method accurately, it is difficult to select an appropriate load increment according to the degree of nonlinearity and to decide suitable smaller load increment near the unknown ultimate state which may be predicted after several trials. Moreover, it is also very difficult to predict the unknown ultimate load and to select the suitable load increment without adequate knowledge and experience. No chance to carry out several trail calculations on the basis of the elasto-plastic and finite displacement theory for deciding the suitable load increment can be permitted in designing actual bridges because of limited computation time and cost.

For these reasons, the arc-length method, shown in Fig. 7, has been introduced into the EPASS on the basis of Refs. 6 and 7. Therefore, the ultimate load of any analytical models can easily be evaluated, because the equilibrium path of the model after reaching their ultimate load points can be traced by using this arc-length method. Each load increment is also decided automatically in this method.

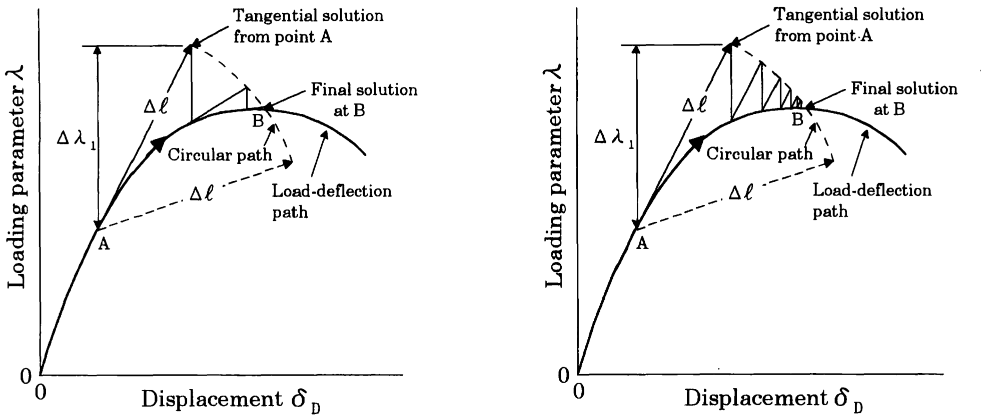

(a) With Newton-Raphson technique (b) With modified Newton-Raphson techique

Fig. 7 Arc-length method

4.2 Current Stiffness Parameter

In order to obtain the ultimate load effectively, a current stiffness parameter (c.s.p.) proposed in Ref. 8 has been adopted. The current stiffness parameter is positive in stable region, negative in unstable region and equal to zero at the stationary points as defined as follows.

The incremental load vector $\Delta \boldsymbol{P}_i$ and the corresponding incremental displacement vector $\Delta \boldsymbol{U}_i$ at the loading level i are standardized by the Euclidean norm of the incremental load vector $|\Delta \boldsymbol{P}_i|$. And the following scalar S_{pi}^* is defined as the reciprocal of the product of these standardized vectors:

$$S_{pi}^* = \frac{|\Delta \boldsymbol{P}_i|^2}{\Delta \boldsymbol{U}_i^T \Delta \boldsymbol{P}_i} \tag{42}$$

This value of S_{pi}^* is in proportion to the stiffness of the analytical model. The current stiffness parameter S_{pi} at the loading level i is defined as:

$$S_{pi} = \frac{S_{pi}^*}{S_{p1}^*} \tag{43}$$

in which S_{p1}^* is the value of S_{pi}^* at the loading level $i = 1$, where the load-displacement relationships of the analytical model under consideration are linear.

Figure 8 shows how the current stiffness parameter changes in accordance with the loading levels in the analysis of a two-hinged arch under a concentrated load[13], as an example. It can be seen from Fig. 8(b) that the current stiffness parameter becomes equal to zero at the extremum

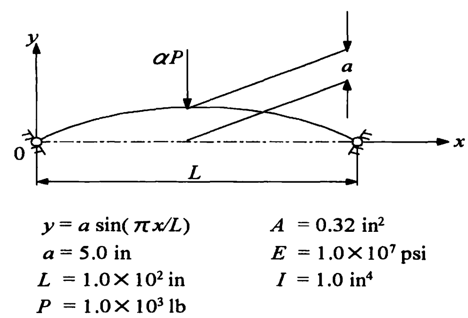

(a) Analytical model

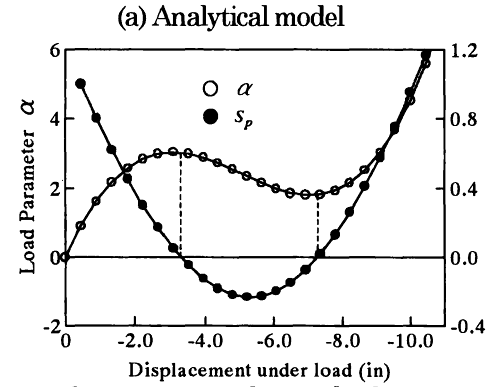

(b) Load parameter and c.s.p.-displacement curves

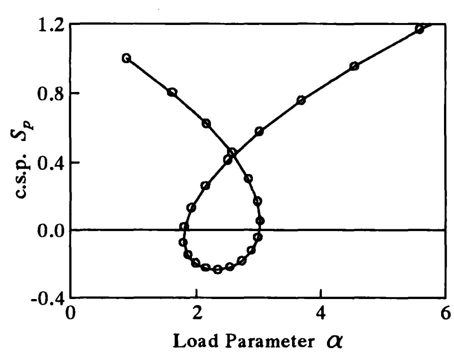

(c) Load parameter-c.s.p. curve

Fig. 8 Current stiffness parameter[5]

points of the load-displacement curve. The ultimate load of the analytical model may be predicted by plotting their current stiffness parameters as shown in Fig. 8(c) and by using the extrapolation in case where the calculation is interrupted before the ultimate state.

4.3 Under-Relaxation Method

The under-relaxation method[9),10)] is adopted in case that the solution will not easily diverge by using constant load increments.

Let us now considered a load increment that the converged configuration of the load step i has been evaluated and the next converged configuration of the load step $i+1$ is going to be calculated. When the solution procedure until the iteration loop k finished, the incremental displacement vector $\Delta \boldsymbol{U}_{i+1}{}^{(k+1)}$ at the iteration loop $k+1$ is expressed as follows:

1) Using load incremental method

$$\Delta \boldsymbol{U}_{i+1}{}^{(k+1)} = \Delta \boldsymbol{U}_{i+1}{}^{(k)} + \beta^{(k+1)}\left[\boldsymbol{K}_{i+1}{}^{(k)}\right]^{-1}\left[\boldsymbol{P}(\lambda_i + \Delta\lambda_{i+1}) - \boldsymbol{F}_{i+1}{}^{(k)}\right] \tag{44}$$

where $\boldsymbol{K}_{i+1}{}^{(k)}$ is the tangent stiffness matrix, $\boldsymbol{P}(\lambda_i + \Delta\lambda_{i+1})$ is the nodal force vector for the external loads, $\boldsymbol{F}_{i+1}{}^{(k)}$ is the nodal force vector for the internal forces, $\Delta\lambda_{i+1}$ is the incremental loading parameter, and $\beta^{(k+1)}$ is the relaxation parameter $(0 < \beta \leq 1)$.

2) Using Arc-length method

$$\Delta \boldsymbol{U}_{i+1}{}^{(k+1)} = \beta^{(k+1)}\left(\Delta \boldsymbol{U}_{i+1}{}^{(k)} + \delta^{(k+1)} + \delta\lambda^{(k+1)}\delta_T\right) \tag{45}$$

$$\left(\Delta \boldsymbol{U}_{i+1}{}^{(k)} + \delta^{(k+1)} + \delta\lambda^{(k+1)}\delta_T\right)^T\left(\Delta \boldsymbol{U}_{i+1}{}^{(k)} + \delta^{(k+1)} + \delta\lambda^{(k+1)}\delta_T\right) = (\Delta\ell)^2 \tag{46}$$

where $\Delta\ell$ is the incremental arc-length and

$$\delta^{(k+1)} = \left[\boldsymbol{K}_{i+1}{}^{(k)}\right]^{-1}\left[\boldsymbol{P}(\lambda_i + \Delta\lambda_{i+1}) - \boldsymbol{F}_{i+1}{}^{(k)}\right] \tag{47}$$

$$\delta_T = \left[\boldsymbol{K}_{i+1}{}^{(k)}\right]^{-1}\boldsymbol{q} \tag{48}$$

in which $\boldsymbol{q}$ is the reference nodal force vector for the external loads.

The value of the incremental loading parameter β is varied on each iteration.

Although the number of iteration loop at the load step increases by using the under-relaxation method, the larger load increment can be used. Then, it may be advantageous to use this method in the case of elasto-plastic analysis using the arc-length method.

4.4 Other Effective Strategies

Other effective strategies which are employed in the EPASS are given as follows:

(1) Partial AULD (Approximate Updated Lagrangian Description)

The finite displacement behavior is formulated according to two types of ULD (Updated Lagrangian Description) methods. One is AULD[11)] and the other is Partial AULD. In the AULD, a reference configuration to make the stiffness matrix is defined approximately by a rigid body motion of the undeformed body of the finite element. The Partial AULD is the AULD improved by the concept used in the PULD (Partial ULD)[14)] in which the coordinates of each element are updated only at the beginning of each load step.

It is advantageous to use the AULD in problems where the geometrically nonlinear behavior predominates and to use the Partial AULD in the case where the elasto-plastic behavior predominates by using the arc-length method.

(2) Efficiency of Making Input Data on Residual Stress

In the presented program, the practical residual stress distribution which have been proposed by the first author through their experimental study[15] can be automatically introduced only by designating the material type of steel in order to raise the efficiency of making input data.

(3) Restarting Function of Calculation

The EPASS provides a function of restarting calculation. Even if a calculation is interrupted accidentally and an unexpected result before reaching the ultimate load of the analytical model under consideration is calculated, the calculation can be resumed from the interrupted state by detecting the bugs and removing them.

5. Verification of the Program

In this chapter, several results of numerical examples analyzed by the EPASS are shown to investigate the validity of EPASS program.

5.1 Elasto-plastic Analysis of Folded Beam Subjected to Bending and Torsion

Two cantilever beams connected at their free edges under a concentrated load are analyzed as a numerical example of bending and torsion to examine the validity of the elasto-plastic behavior of the box members as shown in Fig. 9(a). The analytical results of the relationships between the load P and deflection w at a loading point as plotted in Fig. 9(b) agree with the results by Ref. 1. The variations of bending and torsional moments at three nodal points, where the cross section will yield, are shown in Fig. 10. It can be seen from this figure that numerical results by the EPASS vary along the interaction curve of the fully plastic state.

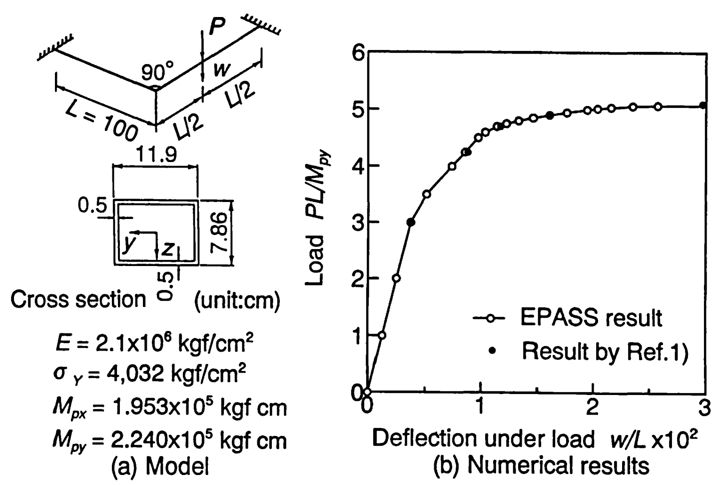

Fig. 9 Analysis of two cantilever beams connected at their free edges[4]

5.2 Elasto-plastic and Finite Displacement Analysis of Column

As a numerical example for elasto-plastic and finite displacement analysis, a box column with the initial deflection and residual stress is analyzed as shown in Fig. 11(a). The obtained results are compared with the Euler's buckling load and the solutions given by Shulz[16] in Fig. 11(b). The ultimate loads obtained by the EPASS agree well with the numerical results by Shulz.

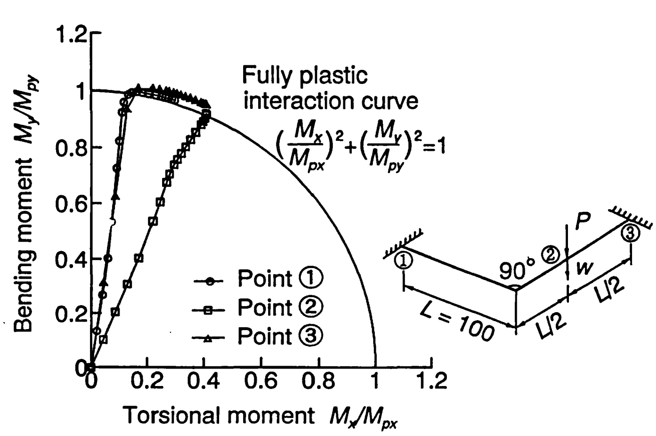

Fig. 10 Interaction between bending moment and torsional moment[4]

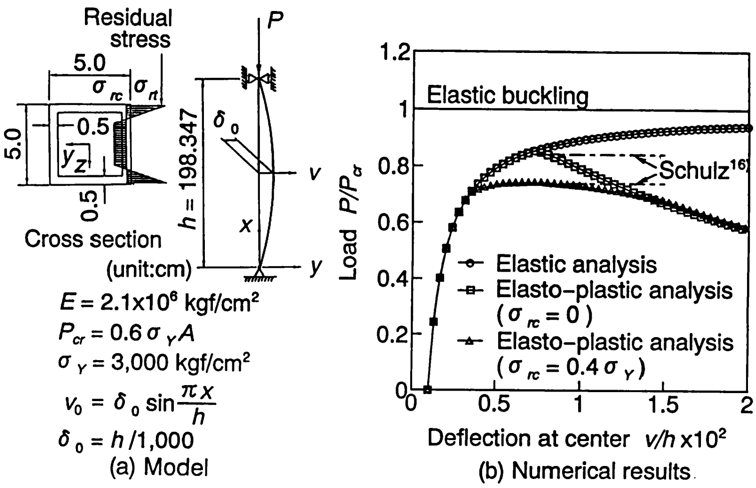

Fig. 11 Analysis of elasto-plastic column with residual stress[4]

6. Practical Example of Cable Stayed Bridge

An actual example of a cable-stayed bridge is analyzed to verify the efficiency of the strategies mentioned above.

6.1 Analytical Model

An analytical model of a cable-stayed bridge[17] with the multi-cable type is shown in Fig. 12. In this model, only the pylons are idealized as the assemblies of elasto-plastic box beam-column elements, which can simulate the elasto-plastic and finite displacement behavior of steel members subjected to the combinations of bending, compression and torsion because the purpose of the analysis is to evaluate the ultimate load carrying capacity of these pylons. Then, the main girder and cables are idealized with the elastic beam-column elements and the elastic rod elements, respectively.

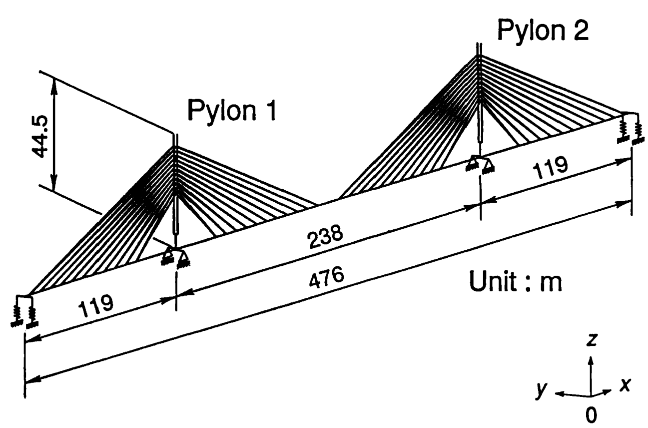

Fig. 12 Analytical model of cable stayed bridge

The residual stress distribution depicted in Fig. 13 is automatically introduced into the cross section of the pylons.

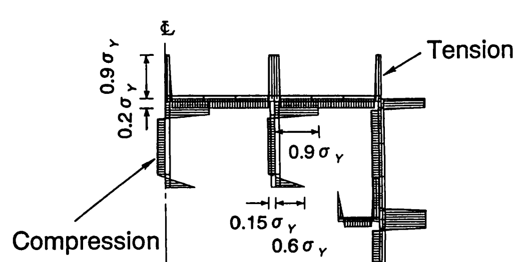

Fig. 13 Residual stress distribution Introduced into cross section of pylons

The load condition applied to the analytical model is defined as follows:

$$1.0(D_1 + P_S + D_2) + 0.7(D_1 + D_2) + \alpha L \quad (49)$$

where

D_1 : pre-dead load (weight of main girder, deck plates and pylons)

D_2 : post-dead load (weight of pavement etc.)

P_S : prestressing forces of cables
L : live load specified by JSHB[18]
α : load parameter to control loading levels

The elasto-plastic and finite displacement analysis is executed according to the following manners. Firstly, the expected initial configuration of the analytical model subjected to the load $1.0(D_1 + P_S + D_2)$ is generated by the method mentioned in the following Section 6.2. Secondly, the load $0.7(D_1 + D_2)$ is applied to this model. Finally, the live load αL is gradually increased up to the ultimate state of the analytical model. $1.7(= 1.0 + 0.7)$ is the safety factor expected in Japan Specifications for Highway Bridges[18].

6.2 Pre-processing Analysis

Pre-processing elastic linear analyses are carried out for evaluating the expected initial configuration of the analysis model subjected to the dead load $(D_1 + D_2)$ and the prestressing forces P_S as shown in Fig. 14. In this case, the stress-resultants of each element are evaluated in the following three analytical models:

1) in the erection model subjected to the pre-dead load D_1,
2) in the erection model without cables subjected to the external forces equivalent to the prestressing forces P_S and
3) in the completion model subjected to the post-dead load D_2

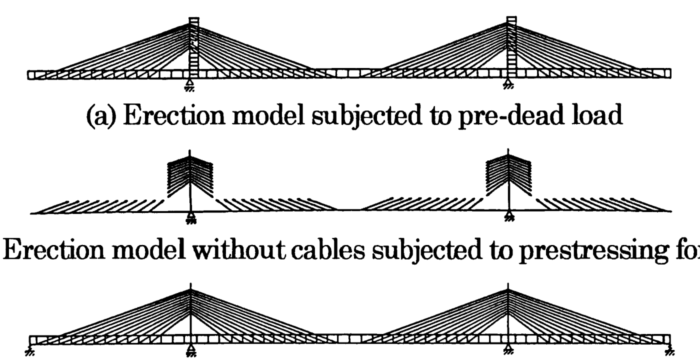

(a) Erection model subjected to pre-dead load

(b) Erection model without cables subjected to prestressing forces

(c) Completion model subjected to post-dead load

Fig. 14 Three models for pre-processing analysis

Then, the obtained stress-resultants are introduced as the initial ones into the completion model together with the dead load $(D_1 + D_2)$ as the initial load and with the prestressing forces P_S as the initial stress-resultants in the cable elements. The expected initial configuration of the completion model can be generated in this method because these initial stress-resultants including the prestressing forces P_S in the cable elements are balanced with the initial load $(D_1 + D_2)$.

6.3 Analytical Results

The numerical results of the analytical model subjected to the live load only on the center span are shown in Figs. 15~18.

Figure 15 shows the relationships between the load parameter and deflection of the top of the Pylon 2. Although the ultimate load may be evaluated from the gradient of the load parameter-deflection curve in the case of the load incremental method, it can be seen that the ultimate load can be obtained accurately by the arc-length method with the under-relaxation method. However, the converged solutions were not obtained near the ultimate load point in the analysis only using the arc-length method.

Figure 16 depicts the relationship between the load parameter and the current stiffness parameter in the load incremental method. In this figure, the ultimate load can be predicted through the extrapolation of

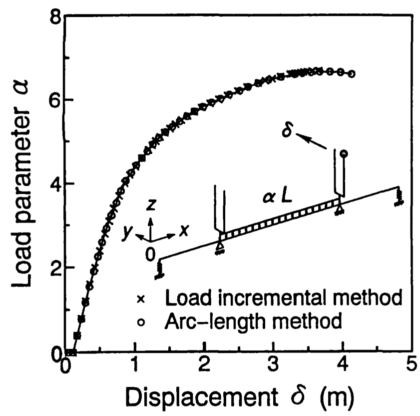

Fig. 15 Load-displacement curves of top of Pylon 2[5)]

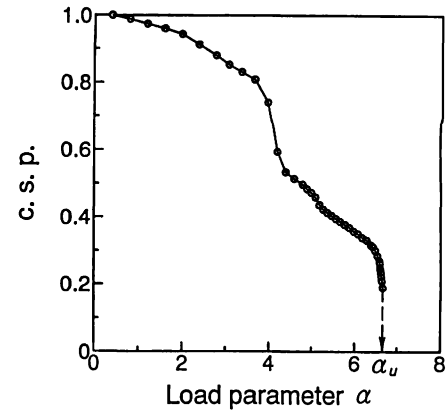

Fig. 16 Prediction of ultimate load by c.s.p.[5)]

the load parameter-c.s.p. curve. As compared Fig. 15 with Fig. 16, it can be seen that this prediction technique of the ultimate load is very effective. And it is possible by using a load parameter-c.s.p. diagram to know how close the final load level to the unknown ultimate load and to ascertain the accuracy of ultimate load obtained by the ordinary load incremental method.

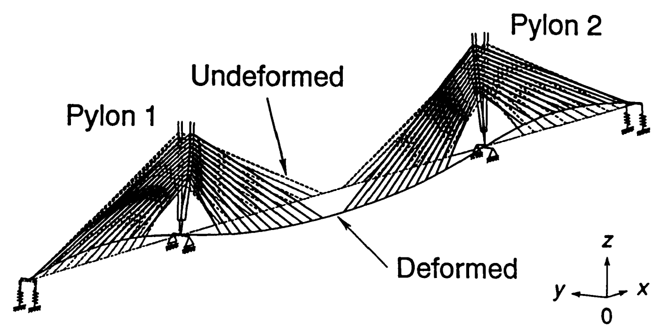

Fig. 17 Deformation of analytical model at ultimate state[5)]

Figure 17 illustrates the deformation of the analytical model at the ultimate state. In this ultimate state, the out-of-plane deformation of the Pylon 2 is predominant.

The deformation and plastic zone of the Pylon 2 at the ultimate state are shown in Fig. 18. This figure is very useful to understand the failure mode of the Pylon 2.

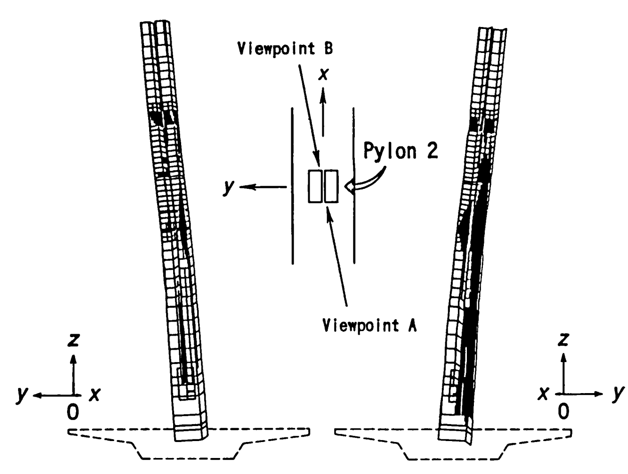

(a) Viewpoint A (b) Viewpoint B

Fig. 18 Deformation and plastic zone of Pylon 2 at ultimate state[5)]

7. Conclusion

In this paper, a computer program, EPASS, to analyze the elasto-plastic and finite displacement behaviors of spatial framed steel bridge structures composed of the thin-walled box members and cable members, have been presented.

The originality of this paper is to formulate the elasto-plastic and finite displacement behavior of beam-column members with box cross section on the basis of a finite element method by taking strain hardening of steel material into consideration.

The validity of the elasto-plastic and finite displacement theory of the thin-walled box members subjected to the combinations of bending, compression and torsion is verified by comparing the numerical results with the theoretical ones and the other numerical ones.

Furthermore, the efficiency of strategies, which are used in the EPASS for the accurate evaluation of the ultimate load, such as the arc-length method, technique by using current stiffness parameter and under-relaxation method, has been verified.

Acknowledgments

The authors would like to express our appreciation to Mr. M. Nibu of Japan Information Processing Service Co., Ltd. and Mr. M. Kano of Bridge & Computer Engineering Co., Ltd. for their cooperation in developing this computer system.

References

1) Komatsu, S. and Sakimoto, T.: Nonlinear Analysis of Spatial Frames Consisting of Members with Closed Cross-Section, Proceedings of Japan Society of Civil Engineers, No. 252, pp. 143-157, August 1976.
2) Maeda, Y. and Hayashi, M.: In-Plane and Out-of-Plane Instability of a 297m Span Steel Arch Bridge, Transportation Research Record 664, Bridge Engineering, Vol. 1, pp. 246-254, September 1978.
3) Nakai, H., Kitada, T., Ohminami, R. and Nishimura, T.: Elasto-Plastic and Finite Displacement Analysis of Cable-Stayed Bridges, Memories of Faculty of Engineering, Osaka City University, Vol. 26, pp. 251-271, December 1985.
4) Tanaka, K., Kitada, T., Nibu, M. and Kano, M.: On a Computer Program, EPASS, to Analyse Ultimate Load Carrying Capacity of Spatial Steel Bridge Structures, Proceedings of Annual Technical Session, Structural Stability Research Council, Milwaukee, Wisconsin, U.S.A., pp. 357-367, April 1993.
5) Kano, M., Kitada, T., Nibu, M. and Tanaka, K.: Effective Strategies for Elasto-Plastic and Finite Displacement Analysis of Spatial Steel Bridges, Proceedings of Annual Technical Session, Structural Stability Research Council, Milwaukee, Wisconsin, U.S.A., pp. 333-343, April 1993.
6) Crisfield, M. A.: A Fast Incremental/Iterative Solution Procedure that Handles "Snap-through", Computers & Structures, Vol. 13, No. 1-3, pp. 55-62, 1981.
7) Bellini, P. X. and Chulya, A.: An Improved Automatic Incremental Algorithm for the Efficient Solution of Nonlinear Finite Element Equations, Computers & Structures, Vol. 26, No. 1/2, pp. 99-110, 1987.
8) Bergan, P. G., Holand, I. and Soreide, T. H.: Use of the Current Stiffness Parameter in Solution of Nonlinear Problems, in Energy Methods in Finite Element Analysis (ed. by Glowinski, R., Rodin, E. Y. and Zienkiewicz, O. C.), John Wiley & Sons, pp. 265-282, 1979.
9) Stricklin, J. A., Haisler, W. E., MacDougall, H. R. and Stebbins, F. J.: Nonlinear Analysis of Shells of Revolution by the Matrix Displacement Method, Journal of American Institute of Aeronautics and Astronautics, Vol. 6, No. 12, pp. 2306-2312, 1968.
10) Kawai, T. and Yoshimura, N.: Analysis of Large Deflection of Plates by the Finite Element Method, International Journal for Numerical Methods in Engineering, Vol. 1, No. 1, pp. 123-133, 1969.
11) Jetteur, P., Cescotto, S. and deGoyet, V.: Improved Nonlinear Finite Element for Oriented Bodies Using an Extension of Marguerre's Theory, Computers & Structures, Vol. 17, No. 1, pp. 129-137, 1983.
12) Goto, S.: Tangent Stiffness Equation of Flexible Cable and Some Considerations, Proceedings of Japan Society of Civil Engineers, No. 270, pp. 41-49, February 1978 (in Japanese).
13) Haisler, W. E. and Stricklin, J. A.: Displacement Incrementation in Non-Linear Structural Analysis by the Self-Correcting Method, International Journal for Numerical Methods in Engineering, Vol. 11, pp. 3-10, 1977.
14) Wong, M. B. and Tin-Loi, F.: Geometrically Nonlinear Analysis of Elastic Framed Structures, Computers & Structures, Vol. 34, No. 4, pp. 633-640, 1990.
15) Komatsu, S., Ushio, M. and Kitada, T.: An Experimental Study on Residual Stresses and Initial Deformations of Stiffened Plates, Proceedings of Japan Society of Civil Engineers, No. 265, pp. 25-35, September 1977 (in Japanese).
16) Schulz, G.: Die Traglastberechnung von Planmäßig Mittig Belasteten Druckstäben aus Baustahl unter Berücksichtigung von Geometrischen und Strukturellen Imperfektionen, Dissertation, T.H. Graz, Juni 1968.
17) Kitada, T., Nakai, H., Kamei, M. and Wakabayashi, Y.: Ultimate Load Capacity of a Cable-Stayed Steel Bridge with Multiple Cables, Proceedings of International Symposium for Innovation in Cable-Stayed Bridge, Fukuoka, Japan, pp. 41-52, April 1991.
18) Japan Road Association: Specifications for Highway Bridges, Part I, Common Specifications and Part II, Steel Bridges, Maruzen, December 1996 (in Japanese).